Sensors and Materials, Vol. 15, No. 1 (2003) 021–035
MYU Tokyo

S & M 0506

Nano-Mechanical Method for Seeding Circular-Shaped Etch Pits on (100) Silicon Surface

Mitsuhiro Shikida, Koji Kawasaki*, Kazuo Sato*, Yasuo Ishihara**, Hiroshi Tanaka** and Akihito Matsumuro*

Research Center for Advanced Waste and Emission Management, Nagoya University
*Department of Micro System Engineering, Nagoya University
**Production Engineering, R & D Department, DENSO CORPORATION

(Received September 13, 2002; accepted January 29, 2003)

Key words: etch pit, anisotropic wet etching, nano-mechanical contact, silicon

We investigated the growth mechanism of circular shallow etch pits appearing on (100) silicon wafers during KOH and TMAH etching, and proved that a very small amount of contact pressure applied to the wafer surface is one source of pit formation on the etched wafer surface. We used nano-indentation equipment to control both contacting force and indentation depth applied to (100) silicon wafers, anisotropically etching the wafers with a 34.0 wt.% KOH solution after forming nanometer-sized indentation marks on them. We found that a square-shaped etch pit appeared at the beginning of the etching process, which gradually became rounder with increased etching time and finally became completely circular in shape. The pit diameter was 80 μm when the etching time was 45 min. In this way, we created artificially controlled circular-shaped etch pits on wafers by nano-mechanical treatment of the wafer surface.

1. Introduction

Anisotropic chemical wet etching is a key technology in fabricating micro-electro-mechanical systems (MEMS). A substantial amount of research has been conducted to understand the etching mechanism and eventually control the etched shape.[1–17] Seidel *et al.*[1,2] and Glembocki *et al.*[3,4] modeled the etching process and investigated the etching properties under a variety of KOH-etching conditions. Tabata *et al.*[7] and Schnakenberg *et al.*[8] investigated the etching properties of a TMAH solution. This solution attacks silicon dioxide film as an etching-mask material in a barely noticeable way and does not contain

ions that can damage the circuits already existing on a wafer.

Circular-shaped shallow etch pits unexpectedly appeared on a (100) silicon wafer during KOH and TMAH etching. The depth of the pits was usually less than 10 μm, and the pits resemble a dimple on the surface of a golf ball. The formation of these pits roughens the etched (100) surface, resulting in poor quality of the etched surface. To address this problem, we investigated the growth mechanism of circular-shaped shallow etch pits appearing on (100) silicon wafers during KOH etching.

2. Experimental Method

Figure 1 shows a typical circular-shaped etch pit formed on an etched (100) surface, with a diameter of up to 100 μm. In our studies, we ascertained that a very small amount of contact pressure applied to the wafer surface is one source of pit formation on an etched wafer surface.

We used nano-indentation equipment in our experiments to control both contacting force and indentation depth applied to (100) silicon wafers. We mainly used a Berkovich-type indenter with a triangular pyramid tip. Since such equipment is usually used for evaluating the hardness and Young's modulus of thin films formed on a substrate, with it we were able to control the contact force and displacement with mN and nm resolution, respectively.

We used CZ-type (100) single crystal silicon chips 14 mm × 14 mm × 0.4 mm in size and with resistivity of 5 – 10 Ωcm. We formed nanometer-sized indentation marks on (100) wafer surfaces, as shown in Fig. 2(a). Figure 2(b) shows a typical mark observed by atomic force microscopy. The indentation depth of the probe was less than 500 nm, and the final size of the indentation marks after releasing the probe from the wafers was less than 300 nm. The applied load was in the range of 10 – 50 mN. We anisotropically etched the wafers with a 34.0 wt.% KOH solution after forming the marks. The etching temperature was 70°C and the etching rate of the (100) plane was 0.55 μm/min.

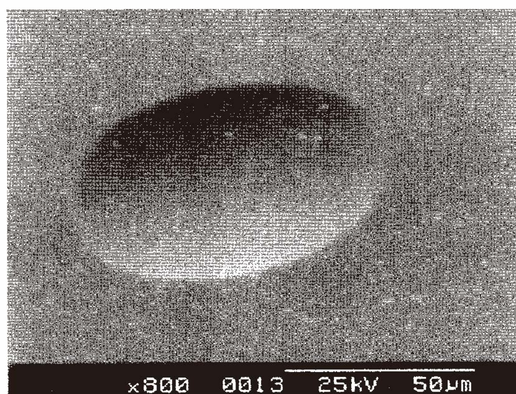

Fig. 1. Circular-shaped etch pit formed on an anisotropically etched (100) wafer.

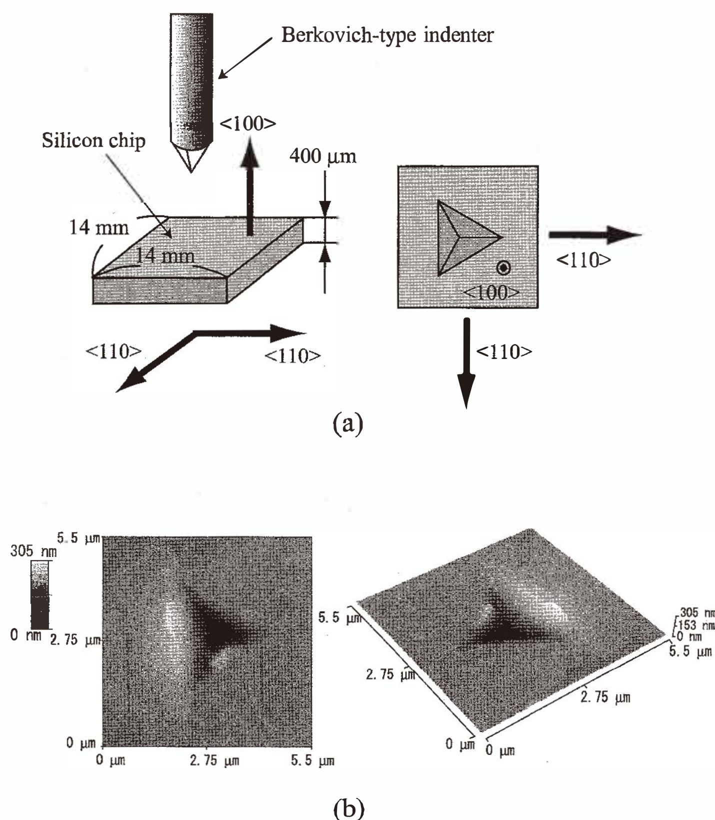

Fig. 2. Nano-indentation applying nanometer-sized marks to the (110) wafer surface. (a) Direction of triangular pyramid tip with respect to crystallographic orientation of the substrate. (b) Nanometer-sized indentation mark observed by atomic force microscopy (Contact force: 50 mN).

3. Experimental Results

3.1 *Circular etch pit formation*

We investigated the changes in etch pit shape that occurred with the forming of indentation marks during the anisotropic etching process. The contact force applied to form the marks was 30 – 50 mN. Figure 3 shows the changes occurring in the marks during the KOH etching process. At first, square-shaped etch pits appeared (Fig. 3(a)) and the size of the etch pits maintaining a square shape became larger with increased etching time (Fig. 3(b)–(c)). After that, the shape of the pits gradually became rounder with increased etching time (Fig. 3(d)–(g)). Finally, the pits became completely circular in shape (Fig. 3(h)). Changes in the etch pit size are shown in Fig. 4. In the figure, we plotted the size change in two different directions. One is the pit width; W, and the other is the length of diagonal direction; D in the etch pit. Both sizes increased with increased etching time. The trend of

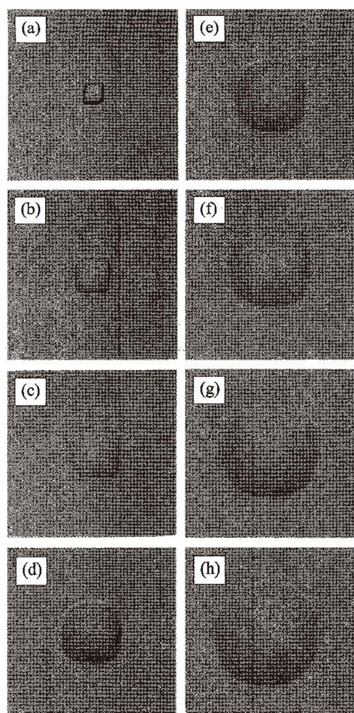

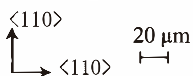

Fig. 3. Change in etch pit shape formed on the (100) wafer during etching (34.0 wt.% KOH, 70°C, contact force: 30 mN). Etching time: (a) 5 min, (b) 10 min, (c) 15 min, (d) 20 min, (e) 25 min, (f) 30 min, (g) 35 min, (h) 45 min.

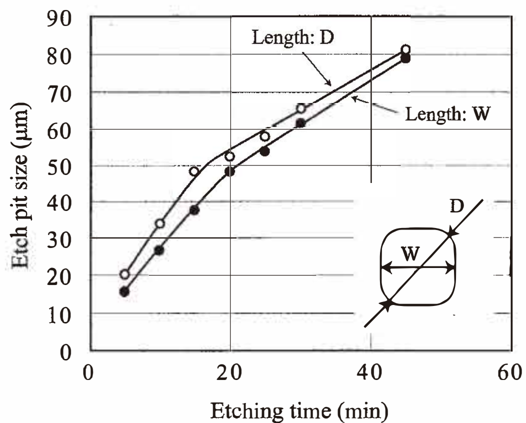

Fig. 4. Change in etch pit size during etching (34.0 wt.% KOH, 70°C, contact force: 50 mN).

the increment of the etch pit size in both directions changed around the etching time of 15–20 min. This point corresponded almost completely to that of the shape change process from square to round, as shown in Fig. 3. Figure 5 shows the change in the pit cross section that occurred during the etching. The pit sidewall was steep in the early stage of the etching, and gradually became flatter as the etching proceeded until it finally became shallow. Figure 6 shows the change in depth that occurred during the etching. During the first 10 minutes, the depth increased sharply to the value of 1.4 μm, and then saturated at that value as the etching continued.

We modeled the shape change of the etch pit during anisotropic etching from the above results.

(1) A square-shaped etch pit appeared at the beginning of the etching, starting from the point of a nanometer-sized indentation mark.
(2) The etch pit grew in size while maintaining a square shape with a constant value of the etch pit depth. As a result, the sidewall of the pit gradually became flat.
(3) When the sidewall became flat, the next etched shape of the pit was determined by the distribution pattern of the etching rate neighboring the (100) direction, the rate of which we assume to be nearly the same as that of the pit. As a result, the square-shaped etch pit started to become round, and finally became circular.

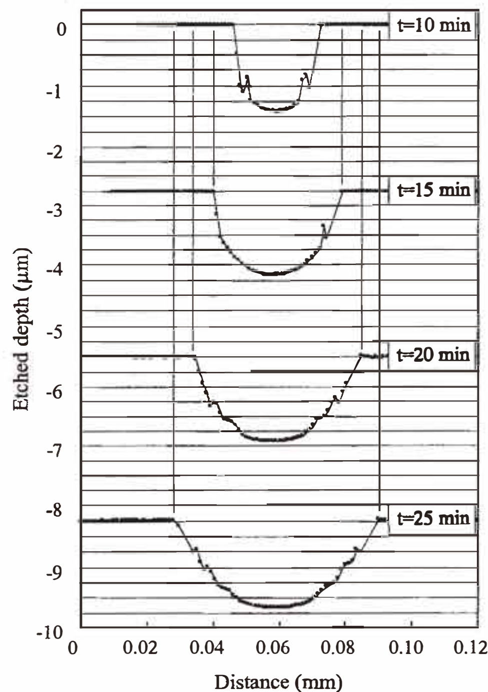

Fig. 5. Change of etch pit cross section during KOH etching (34.0 wt.% KOH, 70°C, contact force: 50 mN).

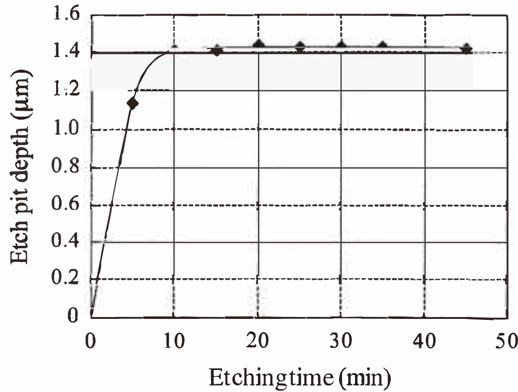

Fig. 6. Change in etch pit depth during etching (34.0 wt.% KOH, 70°C, contact force: 50 mN).

3.2 *Contact force dependence*

We studied the contact force dependence on the formation of circular etch pits. Figures 7 and 8 respectively show the contact force dependence on the etch pit diameter and depth. The etching time was 45 min in the experiments. For this dependence, we obtained the following results.

(1) Etch pit diameter and depth depended on the amount of contact force applied, increasing with increased contact force.

(2) Reproducibility for the etch pit size depended on the amount of contact force applied. High reproducibility was obtained with large contact force.

(3) No etch pits appeared when the contact force was low. Among twelve points of the nano-indentation marks on the silicon surface with a 20 mN contact force, only three of them grew into circular etch pits during etching. No pit growth was observed by an optical microscope in any of the other nine points. When the contact force was 10 mN, no pit growth was observed at any of the indentation points. We therefore believe that etch pit formation can be avoided by handling silicon wafers with low contact force in automated wafer handling systems in production lines.

3.3 *TMAH etching*

The KOH we used in our experiments is the most popular etching solution for fabricating microstructures in micro-electro-mechanical systems because of its high reproducibility, low cost, and large dependency on crystallographic orientation. Currently, however, TMAH is becoming a popular alternative because of its compatibility with integrated circuits fabricated on silicon wafers. We therefore investigated to see if the phenomena that occur with KOH also occur with TMAH. In this investigation, the applied contact force was 50 mN, the TMAH solution concentration was 25.0 wt.%, and the etching temperature was 70°C. The etching rate of the (100) plane was 0.28 μm/min.

Figure 9 shows the changes in etch pit shape that occurred during the TMAH etching

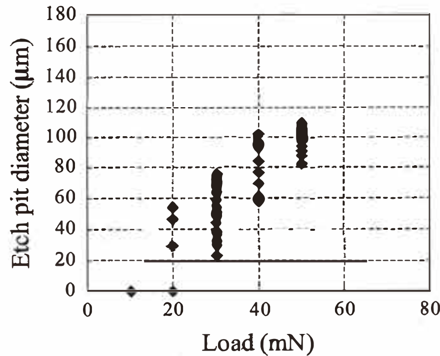

Fig. 7. Contact force dependence on etch pit diameter (34.0 wt.% KOH, 70°C).

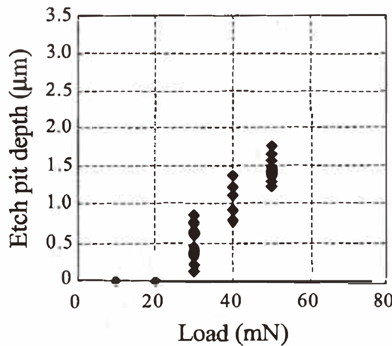

Fig. 8. Contact force dependence on etch pit depth (34.0 wt.% KOH, 70°C).

process. The results were similar to those obtained with KOH etching. At first, square-shaped etch pits appeared (Fig. 9(a)) and then the side of the pits gradually became a gentle slope with increased etching time (Figs. 9(b)–(f)). Though the outline remained rather square-shaped because of the difference in anisotropic nature between KOH and TMAH, the pits gradually became rounded and finally completely circular in shape (Figs. 9(g)–(j)). The final pit diameter was about 200 μm when the etching time was 190 min.

Figure 10 shows the change of the etch pit size that occurred during the TMAH etching. During the first 20 minutes, the depth increased sharply to the value of 1.22 μm, and then saturated at that value as the etching continued (Fig. 10(a)). The etch pit depth was almost the same when the contact force was the same, even if the etching solutions were different. That is, the etch pit depth did not depend on the etching solutions. Figure 10(b) shows the change in the etch pit size. As seen in the figure, the size in both directions increased with increased etching time. The trend of the increment of the etch pit size in both directions changed around the etching time of 30–50 min. These phenomena are consistent with the results obtained for KOH etching.

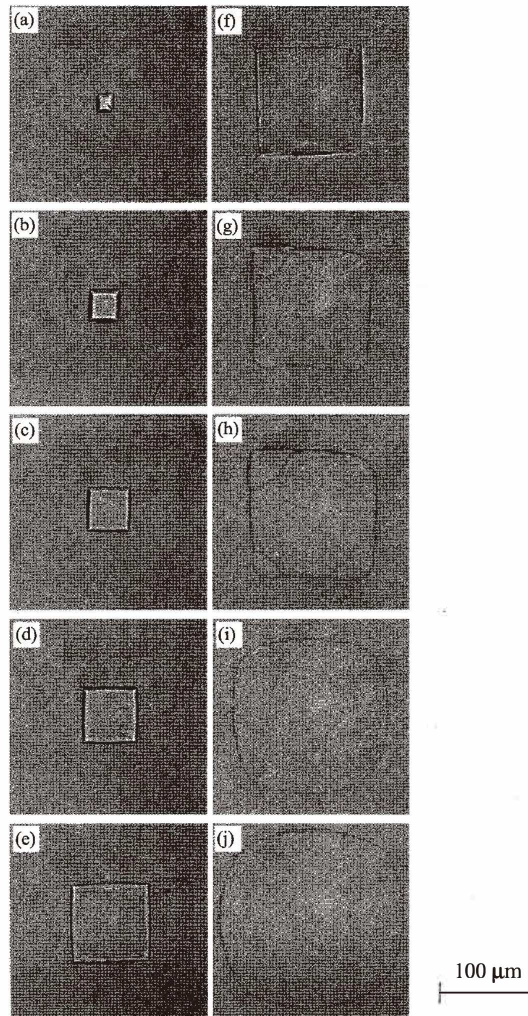

Fig. 9. Change in etch pit shape during TMAH etching (25.0 wt.% TMAH, 70˚C, contact force: 50 mN). Etching time: (a) 5 min, (b) 10 min, (c) 15 min, (d) 20 min, (e) 30 min, (f) 50 min, (g) 80 min, (h) 100 min, (i) 160 min, (j) 190 min.

4. Model of Circular Etch Pit Formation

We believe that the model of the circular etch pit growth is as follows (Fig. 11).

(1) Induction of crystal dislocation into silicon wafer

Mechanical contact with nano-indentation induced dislocations into single-crystal silicon wafer surfaces. As shown in Figs. 11(a)–(b), dislocations were induced around

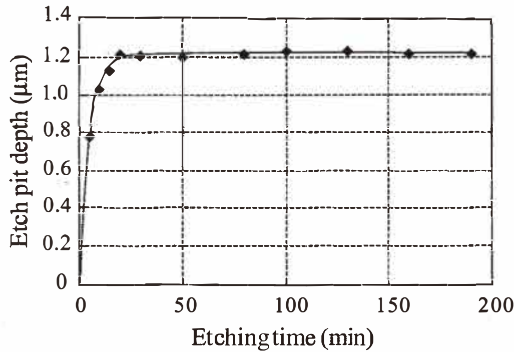

(a) Depth

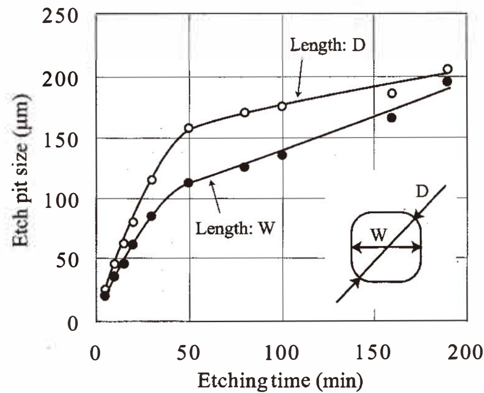

(b) Size

Fig. 10. Change in etch pit size during TMAH etching (25.0 wt.% TMAH, 70°C, contact force: 50 mN).

nanometer-sized marks, in planes with the highest atomic density. They therefore exist on the (111) plane and propagate in the direction of the (110) orientation for single-crystal silicon. The (111) planes are located at an angle of 54.7° to the (100) wafer surface.

(2) Square-shaped etch pit formation

The imperfectness of the crystal regions containing an induced dislocation was rapidly removed at the beginning of the etching process (Fig. 11(c)). This therefore indicates square-shaped etch pits were formed on the (100) surface according to the location of (111) planes containing dislocations. The directions of the four sides of square-shaped etch pits correspond to those of (111) appearing on the wafer surface.

The shape of square-shaped etch pits did not depend on the tip shape of the indenter. Figure 12 shows the change in the indentation mark formed by a spherical-shaped tip during KOH etching. We obtained the same results even if we used a different-shaped indenter tip. Furthermore, the etch pit depth did not depend on the etching solutions, but on

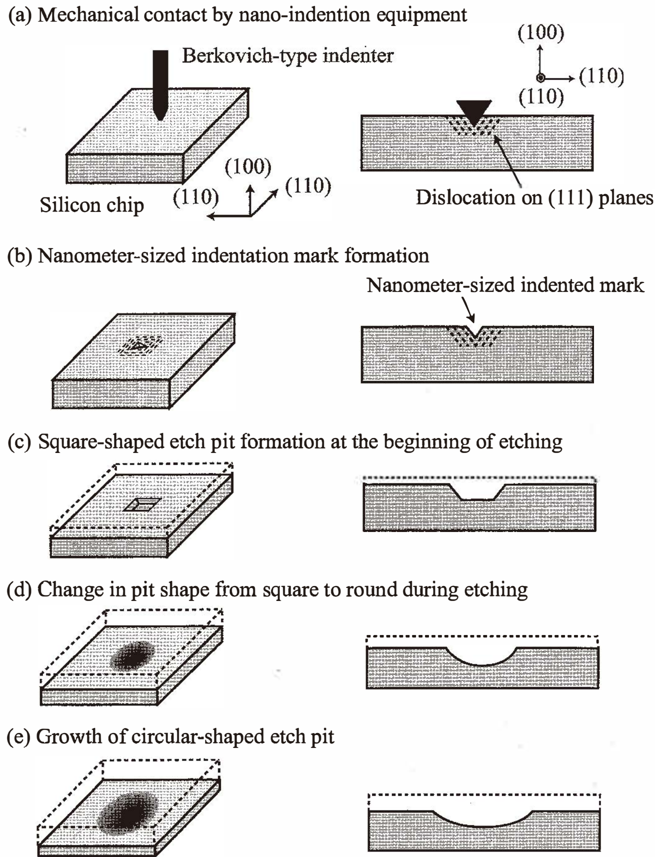

Fig. 11. Model of circular etch pit formation starting from nanometer-sized defect.

the amount of the applied contact force.

We therefore believe that square-shaped etch pit formation on the (100) plane at the beginning of the etching process is due to dislocations induced as a result of mechanical contact.

(3) Circular-shaped etch pit formation

The square-shaped etch pits gradually became rounded according to the distribution pattern of the etching rate around the (100) orientation (Fig. 11(d)–(e)). To confirm this, we artificially formed a trapezoid-shaped hole on the silicon surface, and then etched it with the KOH solution. Figure 13 illustrates this procedure. At first, we deposited a silicon dioxide film and patterned it to form the etching mask (Figs. 13 (a)–(b)). Then, we formed a trapezoid-shaped hole with the depth of 8.3 μm by using KOH etching (Fig. 13 (c)), and then removed the etching mask (Fig. 13(d)). We then applied KOH etching to a chip having a trapezoid-shaped hole to confirm whether the hole became circular or not during

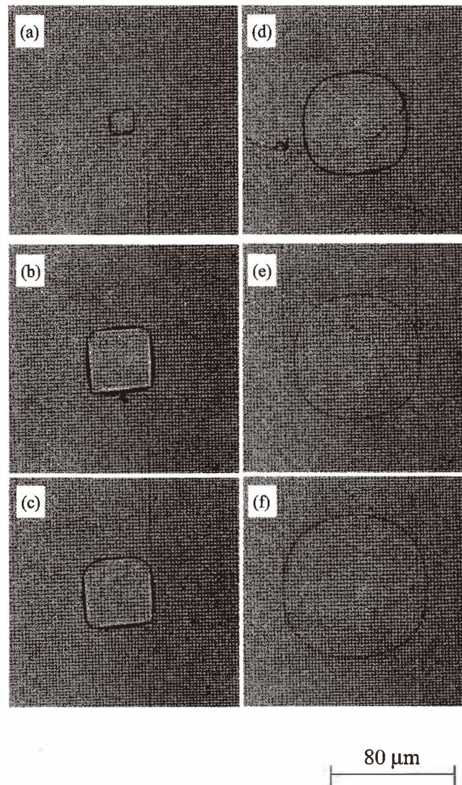

Fig. 12. Change in indentation mark formed by spherical tip during KOH etching (34.0 wt.% KOH, 70 °C, contact force: 50 mN). Etching time: (a) 5 min, (b) 10 min, (c) 15 min, (d) 25 min, (e) 35 min, (f) 45 min.

KOH etching (Figs. 13(e)–(f)). Figure 14 shows the experimental results for the change in the shape of the trapezoid-shaped hole during KOH etching. It can be seen that the shape gradually changed from square to circular. We therefore think that this process is dominated by the anisotropic nature of the etching, and that etching rates around the (100) direction are almost the same for all cases.

5. Nano-Indentation Etching Method Application

Circular etch pits can be artificially created on a wafer by nano-mechanical treatment of the wafer surface. To demonstrate this, we artificially fabricated circular pits at arbitrarily tailored locations. Figure 14 shows examples of circular etch pits formed by nano-indentation marks followed by the KOH etching process, with applied force of 50 mN. The KOH concentration was 34.0 wt.% and the etching temperature was 70°C.

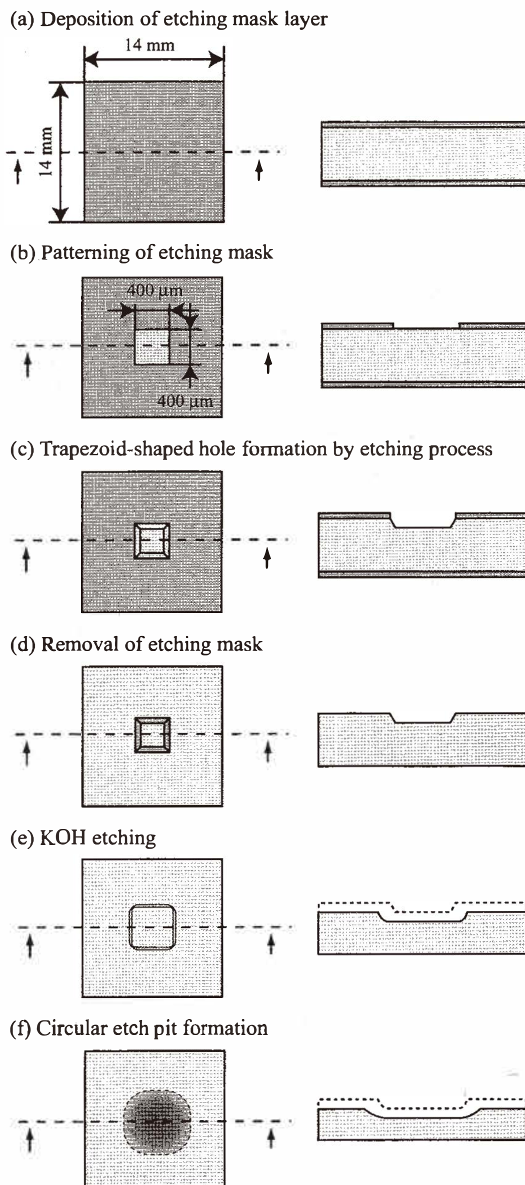

Fig. 13. Procedure to confirm the change in artificially formed trapezoid-shaped hole during KOH etching.

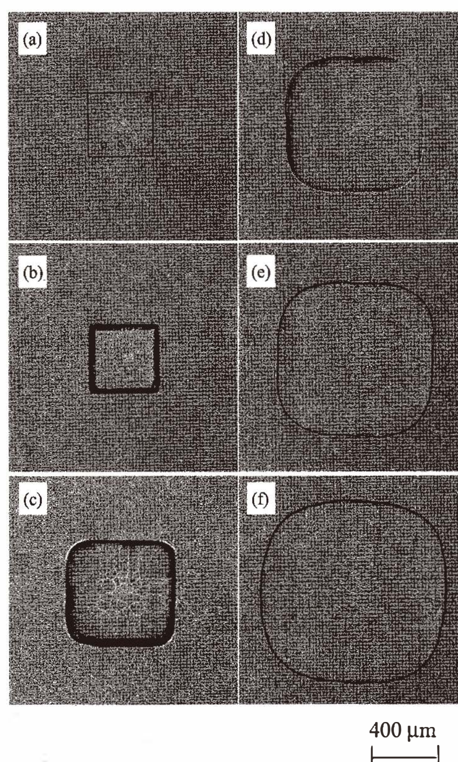

Fig. 14. Change in artificially formed trapezoid-shaped hole during KOH etching (34.0 wt.% KOH, 70°C, contact force: 50 mN). Etching time: (a) 0 min, (b) 45 min, (c) 135 min, (d) 255 min, (e) 360 min, (f) 460 min.

6. Conclusion

We investigated the mechanism of circular pit formation on (100) Si and obtained the following results.

(1) We proved that a very small amount of contact pressure applied to an etched wafer surface is one source of pit formation on the surface. This means that to eliminate circular etch pits, it is essential to avoid mechanical contact with the wafer surface during wafer handling prior to etching.

(2) Square-shaped etch pits appeared at the beginning of the etching process, starting from the point of nanometer-sized indentation marks. They gradually became rounder with increased etching time, finally becoming completely circular in shape.

(3) The size of the etch pits formed by KOH etching depended on the contact force, decreasing with decreased contact force. No pits appeared under a low contact force of less than 10–20 mN.

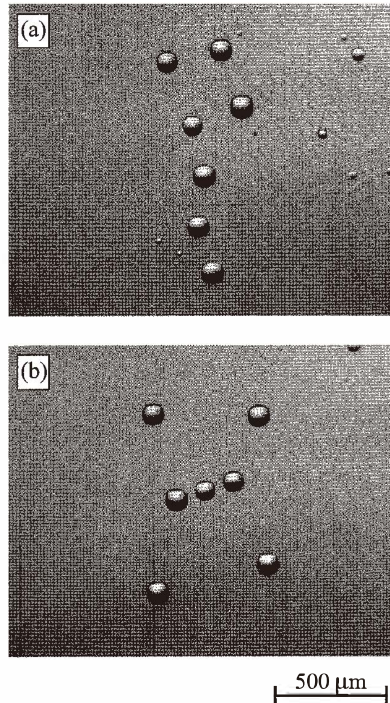

Fig. 15. Artificially controlled patterns of arrayed circular-shaped etch pits. (a) Ursa Major, (b) Orion.

(4) Circular etch pits were formed during both the KOH and TMAH etching processes.
(5) We created an artificially-controlled shallow etch profile on wafers through nano-mechanical treatment of the wafer surface.

Acknowledgement

This work was partially supported by a Grant-in-Aid for the Encouragement of Young Scientists No. 13750216 from the Ministry of Education, Culture, Sports, Science and Technology, and a grant from the Toyota Physical and Chemical Research Institute.

References

1 H. Seidel, L. Csepregi, A. Heuberger and H. Baumgärtel: J. Electrochem. Soc. **137** (1990) 3612.
2 H. Seidel: Tech. Digest of Transducers '87 (1987) p. 120.
3 O. J. Glembocki, E. D. Palik, G. R. de Guel and D. L. Kendall: J. Electrochem. Soc. **138** (1991) 1055.

4 E. D. Palik, O. J. Glembocki, I. Heard, Jr. P. S. Burno and L. Tenerz: J. Appl. Phys. **70** (1991) 3291.
5 L. D. Clark Jr. and D. J. Edell: Proc. of IEEE Micro-Robots and Teleoperators Workshop (1987).
6 P. M. Zavracky: Electrochem. Soc. Proc. 97-**5** (1997) 102.
7 O. Tabata, R. Asahi, H. Funabashi, K. Shimaoka and S. Sugiya: Sensors and Actuators A **34** (1992) 51.
8 U. Schnakenberg, W. Benecke and P. Lange: Tech. Digest of Transducers '91 (1991) p. 815.
9 A. Koide, K. Sato and S. Tanaka: Proc. of IEEE Micro Electro Mechanical Systems (MEMS) Workshop (1991) 216.
10 A. Koide, K. Sato, S. Suzuki and M. Miki: Tech. Digest 11th Sensor Symposium (1992) p. 23.
11 A. Koide and S. Tanaka: Proc. of IEEE MEMS Workshop (1997) p. 418.
12 J. Fr¸hauf and B. Hannemann: J. Micromech. Microeng. **7** (1997) 137.
13 C. R. Tellier and S. Durand: Sensors & Actuators A **60** (1997) 168.
14 G. Schr^pfer, M de Labachelerie and C. R. Tellier: Microsystem Technologies 5 (1999) 194.
15 K. Sato, M. Shikida, T. Yamashiro, K. Asaumi, Y. Iriye and M. Yamamoto: Sensors & Actuators A **73** (1999) 131.
16 M. Shikida, K. Sato, K. Tokoro and D. Uchikawa: Sensors & Actuators A **80** (2000) 179.
17 K. Asaumi, Y. Iriye and K. Sato: Proc. of IEEE MEMS Workshop (1997) p. 412.